# *In situ* studies of reversible solid-gas reactions of ethylene responsive silver pyrazolates

H. V. Rasika Dias,[1,*] Devaborniny Parasar,[1] Andrey A. Yakovenko,[2,*] Peter W. Stephens,[3,*] Álvaro R. Muñoz-Castro,[4,*] Mukundam Vanga,[1] Pavel Mykhailiuk,[5,6] Evgeniy Slobodyanyuk[5]

[1] Department of Chemistry and Biochemistry, The University of Texas at Arlington, Arlington, Texas 76019, United States; [2] X-Ray Science Division, Advanced Photon Source, Argonne National Laboratory, Argonne, Illinois 60439, United States; [3] Department of Physics and Astronomy, Stony Brook University, Stony Brook, NY 11794-3800, United States; [4] Facultad de Ingeniería, Arquitectura y Diseño, Universidad San Sebastián, Bellavista 7, Santiago, 8420524, Chile; [5] Enamine Ltd., Winston Churchill Street 78, 02094 Kyiv, Ukraine; [6] Taras Shevchenko National University of Kyiv, Faculty of Chemistry; Volodymyrska 60, 01601 Kyiv, Ukraine

*Email:*
*dias@uta.edu; ayakovenko@anl.gov; peter.stephens@stonybrook.edu; alvaro.munozc@uss.cl*

**Abstract.**

Solid-gas reactions and *in situ* powder X-ray diffraction investigations of trinuclear silver complexes {[3,4,5-$(CF_3)_3$Pz]Ag}$_3$ and {[4-Br-3,5-$(CF_3)_2$Pz]Ag}$_3$ supported by highly fluorinated pyrazolates reveal that they undergo intricate ethylene-triggered structural transformations in the solid-state producing dinuclear silver-ethylene adducts. Despite the complexity, the chemistry is reversible producing precursor trimers with the loss of ethylene. Less reactive {[3,5-$(CF_3)_2$Pz]Ag}$_3$ under ethylene pressure and low-temperature conditions stops at an unusual silver-ethylene complex in the trinuclear state, which could serve as a model for intermediates likely present in more common trimer-dimer reorganizations described above. Complete structural data of three novel silver-ethylene complexes are presented together with a thorough computational analysis of the mechanism.

## Introduction

Trinuclear silver(I) complexes of fluorinated pyrazolates have attracted significant interest because many of them show interesting π-acid properties, luminescence, argentophilic contacts, and useful applications.[1-8] For example, {[3,5-$(CF_3)_2$Pz]Ag}$_3$ (Figure 1, **[Ag-H]$_3$**) reported by one of us,[9] is a strong π-acid and display rich π-acid/π-base chemistry with unsaturated hydrocarbons leading to sandwich complexes of various types.[10] It also serves as a sensor for arenes such as benzene and toluene.[11, 12] With *o*-terphenyl,[13] it produces a white light emitting material while the treatment of **[Ag-H]$_3$** with phenylacetylene produces a $Ag_{13}$ cluster with the breakup of the $Ag_3N_6$ core.[14] The silver complex has also been utilized in the desulfurization of fossil fuels.[15]

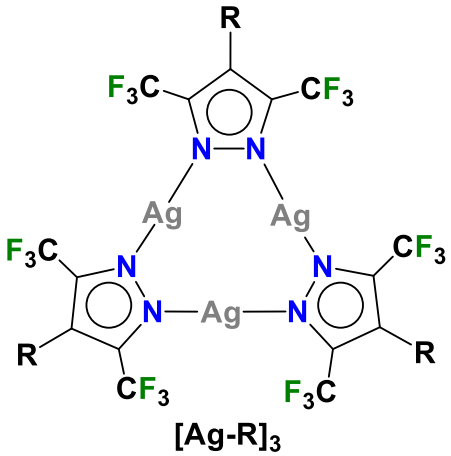


**Figure 1.** Trinuclear silver(I)-pyrazolates utilized in this work, {[4-R-3,5-$(CF_3)_2$Pz]Ag}$_3$ (**[Ag-R]$_3$**, R = H, Br, $CF_3$)

In contrast to the aromatic hydrocarbons, the chemistry of industrially relevant gaseous hydrocarbons such as ethylene with silver pyrazolates has not been explored. Silver-ethylene complexes are of particular interest since silver is the metal of choice for partial oxidation of ethylene, which is a major industrial process.[16, 17] They are challenging to stabilize and quite labile due to the relatively weak silver(I)-ethylene interactions.[18-24] Reversible binding of ethylene to silver, however, is valuable in applications such as the separation of ethylene from ethylene-ethane mixtures using silver complexes and silver-doped materials.[25-27] The copper(I) analogs of **[Ag-H]$_3$** such as {[4-R-3,5-$(CF_3)_2$Pz]Cu}$_3$ (**[Cu-R]$_3$,** R = H, $CF_3$) are effective in the selective separation of ethylene from ethane containing mixtures.[28, 29]

Motivated by the fundamental interest and novelty, we embarked on an in-depth study of ethylene chemistry of silver(I) pyrazolates {[4-R-3,5-$(CF_3)_2$Pz]Ag}$_3$ (**[Ag-R]$_3$**, R = H, Br, $CF_3$) with different pyrazolyl ring substituents that also utilizes solid-gas[30-33] synthesis and in situ powder X-ray diffraction (PXRD) measurements at 17-BM beamline at the Argonne National Laboratory (ANL) advanced photon source. As evident from the following account, this undertaking was successful and led to the stabilization of an unusual trinuclear silver-ethylene complex in a crystalline state. We also uncovered two unprecedented dinuclear silver-ethylene

complexes with bridging pyrazolates, of which, only one could be obtained via a traditional solution method.

## Results and Discussion

***Traditional solution chemistry:*** The per-fluorinated silver(I) complex {[3,4,5-$(CF_3)_3$Pz]Ag}$_3$ (**[Ag-$CF_3$]$_3$**) was utilized first for this purpose because it possesses powerful Lewis acidic silver sites and is expected to be more reactive towards ethylene compared to the less-fluorinated analogs. The **[Ag-$CF_3$]$_3$** was obtained very conveniently via a reaction between the corresponding pyrazole [3,4,5-$(CF_3)_3$Pz]H[34] and silver(I) oxide. It is a colorless, air-stable solid and has been characterized by several techniques including NMR spectroscopy, and single crystal and powder X-ray crystallography. It crystallizes with a molecule of dichloromethane in the asymmetric unit (Figure 2, see supporting information for additional details and Figures S7-S8) and displays short intermolecular Ag•••Cl and Ag•••F contacts. There are no argentophilic interactions as observed in **[Ag-H]$_3$** or electron-rich systems like {[3,5-$(Ph)_2$Pz]Ag}$_3$ and {[3,5-(*i*-$Pr)_2$Pz]Ag}$_3$.[35-37]

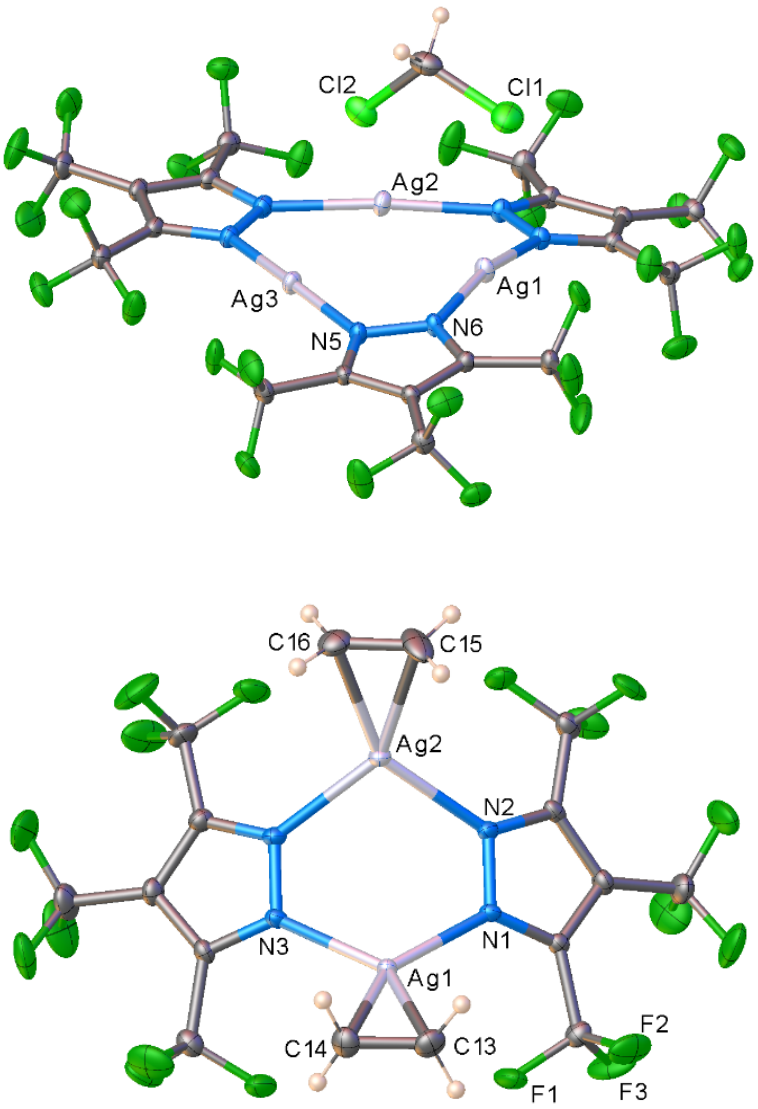


**Figure 2.** Molecular structure of **[Ag-$CF_3$]$_3$•$CH_2Cl_2$** (top) and **[Ag-$CF_3$•($C_2H_4$)]$_2$** (bottom) obtained from solution process and single crystal X-ray diffraction studies.

More importantly, **[Ag-$CF_3$]$_3$** reacts with ethylene in $CH_2Cl_2$ at low temperatures and produces a product which can be crystallized from the same

mixture at -25 °C under an ethylene blanket (Scheme 1). The variable temperature $^{19}F$ NMR spectroscopic data show that this transformation takes place below -10°C in $CD_2Cl_2$. The analysis of crystalline solid using single crystal X-ray diffraction reveals that it is a dinuclear species **[Ag-CF₃•(C₂H₄)]₂** (Figure 2), and a rare isolable silver-ethylene complex.[20, 22, 23, 38-54] Solid samples, however, lose ethylene rapidly upon removal from the ethylene atmosphere at room temperature and return to the ethylene-free trimer form **[Ag-CF₃]₃** (Scheme 1).

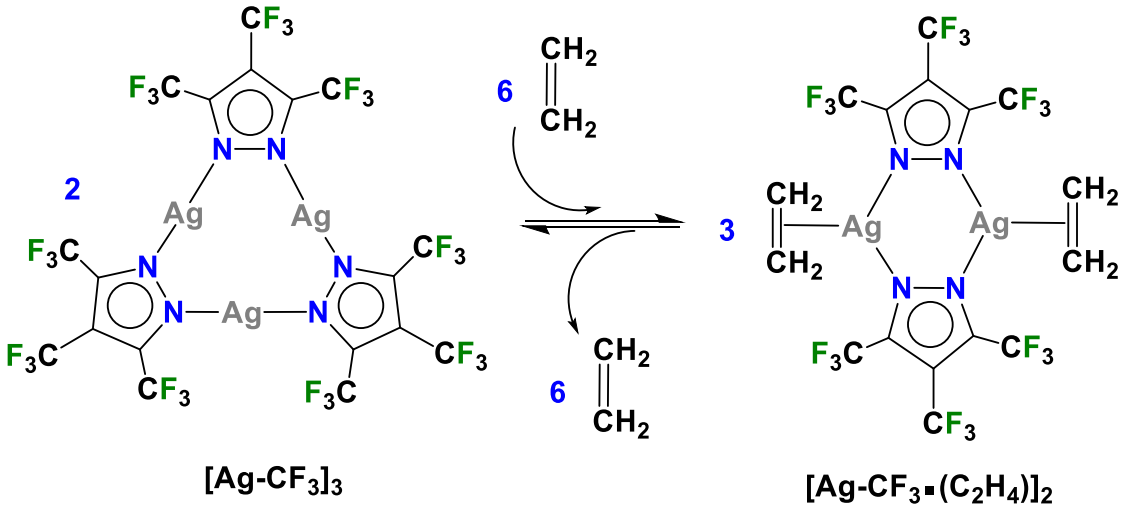


**[Ag-CF₃]₃** **[Ag-CF₃▪(C₂H₄)]₂**

**Scheme 1.** Ethylene responsive trinuclear silver(I)-pyrazolate **[Ag-CF₃]₃** that undergoes structural changes upon addition of ethylene to form **[Ag-CF₃•(C₂H₄)]₂** and reverts to **[Ag-CF₃]₃** upon removal of ethylene.

There are two chemically similar but crystallographically different molecules of **[Ag-$CF_3$•($C_2H_4$)]$_2$** in the asymmetric unit. The silver sites are trigonal planar and $Ag_2N_4$ cores adopt a boat shape. Although there are no analogous dinuclear silver-ethylene complexes for a direct comparison, a few silver-ethylene complexes such as [PhB(3-($CF_3$)Pz)$_3$]Ag($C_2H_4$)[41] and {[$H_2$C(3,5-($CF_3$)$_2$Pz)$_2$]Ag($C_2H_4$)}[$SbF_6$][20] with a three coordinate silver sites supported by N-donor ligands are known. The average Ag-N (2.231 Å) and Ag-C (2.282 Å) distances of **[Ag-$CF_3$•($C_2H_4$)]$_2$** are similar to those observed in [PhB(3-($CF_3$)Pz)$_3$]Ag($C_2H_4$) (av. Ag-N and Ag-C are 2.261 and 2.264 Å, respectively).

Next, we focussed on the related {[3,5-($CF_3$)$_2$Pz]Ag}$_3$ (**[Ag-H]$_3$**),[9] which is a molecule based on less fluorinated pyrazolate possessing relatively less electrophilic silver sites. Our attempts to observe the silver-ethylene complex from a reaction between **[Ag-H]$_3$** and ethylene in $CH_2Cl_2$ solution were unsuccessful even at -50°C. It is understandable since ethylene-silver bonds in general are quite weak while the Ag-N bonds in **[Ag-H]$_3$** are relatively strong considering that it features a better electron-donating pyrazolate[55] than the one present in **[Ag-$CF_3$]$_3$**.

***In situ solid-gas chemistry**:* We then decided to investigate these processes, using solid materials and study the progress of the reaction "live" using *in situ* PXRD at ANL synchrotron beamline. Recent developments show that *in situ, in crystallo,* and solid-gas chemistry are valuable techniques that enable synthesis and characterization of organometallic species that are difficult or impossible to observe under solution-phase conditions.[30-33] Remarkably, crystals of **[Ag-$CF_3$]$_3$** upon exposure to ethylene (3-5 bar at 295K, Figure S10), converted smoothly to the same dinuclear silver-ethylene complex **[Ag-$CF_3$•($C_2H_4$)]$_2$** (Figures S13), mimicking process that occurs in solution. The PXRD based molecular structure of the solid-gas generated **[Ag-$CF_3$•($C_2H_4$)]$_2$** is very similar to that obtained from traditional solution chemistry (and single crystal X-ray crystallography, Figure 2). It is a reversible process (as in the solution) and affords ethylene free precursor **[Ag-$CF_3$]$_3$** (Figure 3) upon purging crystalline **[Ag-$CF_3$•($C_2H_4$)]$_2$** with helium at 295K (Figures S11 and S14). Furthermore, these solid-gas reactions, despite the complexity and break-up and formation of several bonds and rearrangement of molecular fragments, are quite fast as evident from the PXRD patterns. Although the progress of both the forward and reverse reaction involving **[Ag-$CF_3$]$_3$** can be followed using in situ PXRD, the trimer-dimer transition under the conditions noted

above generates the products directly with no evidence of crystalline phases attributable to intermediates.

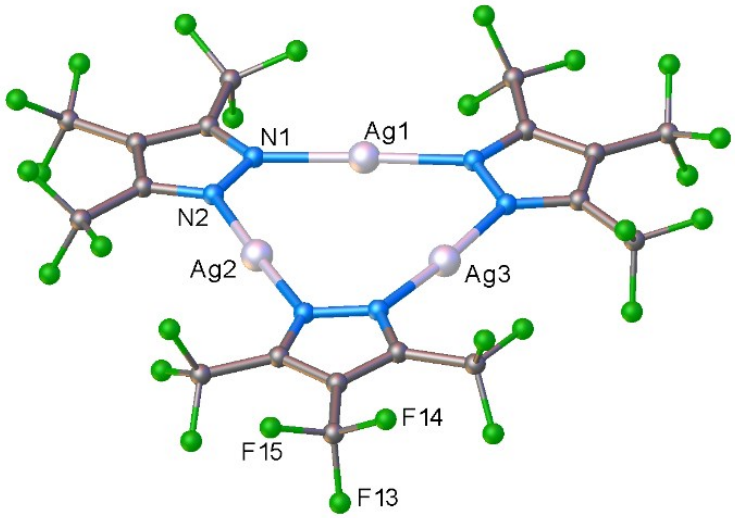


**Figure 3.** Molecular structure of **[Ag-$CF_3$]$_3$** obtained by in situ powder X-ray diffraction studies of the materials from solid-gas chemistry.

To see if we can detect transient species, we proceeded with *in situ* studies of the less reactive **[Ag-H]$_3$** with ethylene. In contrast to **[Ag-$CF_3$]$_3$**, the reaction of solid **[Ag-H]$_3$** with ethylene did not proceed at 295K even under high ethylene pressure up to 60 bar (ESI Figure S16), nor when cooled to 173K under ~1 bar of ethylene flow. However, to our delight, the solid-gas reaction proceeded as we lowered the temperature of polycrystalline **[Ag-H]$_3$** while subjecting the sample to higher ethylene pressure. Specifically, the transformation was evident from the *in situ* PXRD experiment as the PXRD lines of **[Ag-H]$_3$** started to disappear around 223K

at 10 bar (or 206K at 5 bar) of ethylene with the generation of a new crystalline phase (Figures S17 and S19). This new phase does not change even upon further cooling to 173K under ethylene. The process of ethylene uptake by **[Ag-H]$_3$** is reversible, and the product converts back to ethylene free **[Ag-H]$_3$** upon warming to about 262K even under 10 bar of ethylene (Figure S18). The PXRD data analysis revealed the structure of the product (illustrated in Scheme 2), which turned out to be *not the dinuclear species* encountered with **[Ag-CF$_3$]$_3$**, but an unusual silver-ethylene complex {[3,5-(CF$_3$)$_2$Pz]Ag(C$_2$H$_4$)}$_3$ (**[Ag-H•(C$_2$H$_4$)]$_3$**) that retains the trinuclear form.

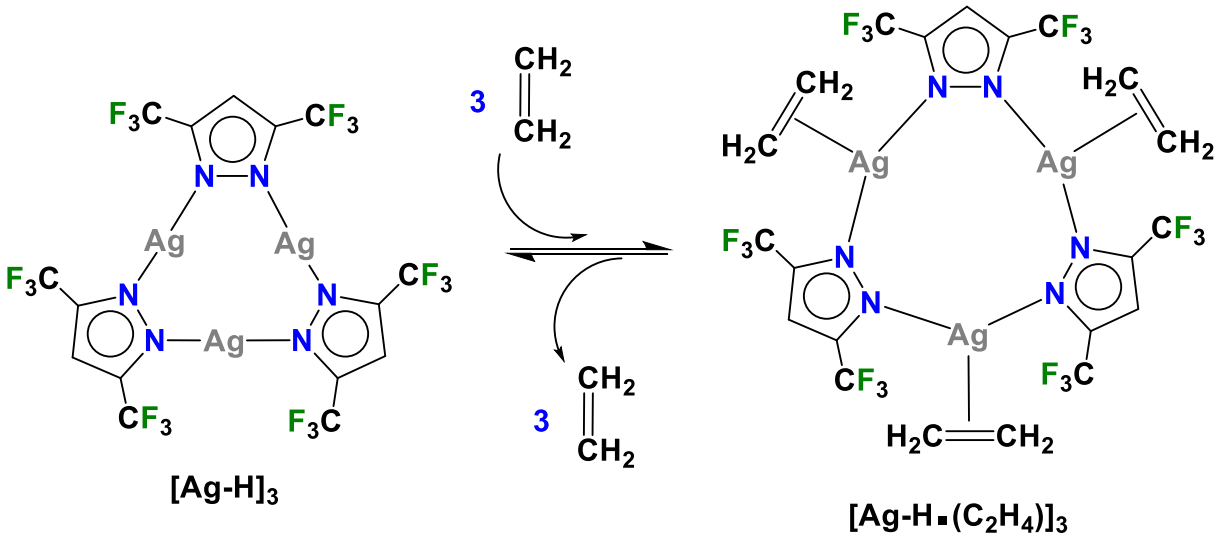


**Scheme 2.** Reaction of **[Ag-H]$_3$** with 10 bar ethylene below temperature of 223 K (or 5 bar of ethylene below 206K) leading the trinuclear silver-ethylene complex {[3,5-(CF$_3$)$_2$Pz]Ag(C$_2$H$_4$)}$_3$ (**[Ag-H•(C$_2$H$_4$)]$_3$**) with a nine-membered Ag$_3$N$_6$ core.

The molecular structure of this unprecedented species **[Ag-H•($C_2H_4$)]$_3$** is illustrated in Figure 4 (and Figure S23). It is a trinuclear silver complex featuring a nine-membered $Ag_3N_6$ metallacycle, and three trigonal-planar silver-ethylene sites. The $Ag_3N_6$ core of **[Ag-H•($C_2H_4$)]$_3$** displays significant puckering compared to the planar configuration found in **[Ag-H]$_3$** (and the related **[Ag-$CF_3$]$_3$**, see Figure 3).[9] This large deviation from planarity is a result of the interaction of ethylene with silver sites from opposite faces, but the interactions are perhaps not strong enough to break the Ag-N bonds at low-temperature conditions. The compound **[Ag-H•($C_2H_4$)]$_3$** may possibly be a model for a likely intermediate present in more facile reaction of **[Ag-$CF_3$]$_3$** with ethylene, just prior to the breakup of trimers to produce the corresponding dinuclear metal-ethylene complexes.

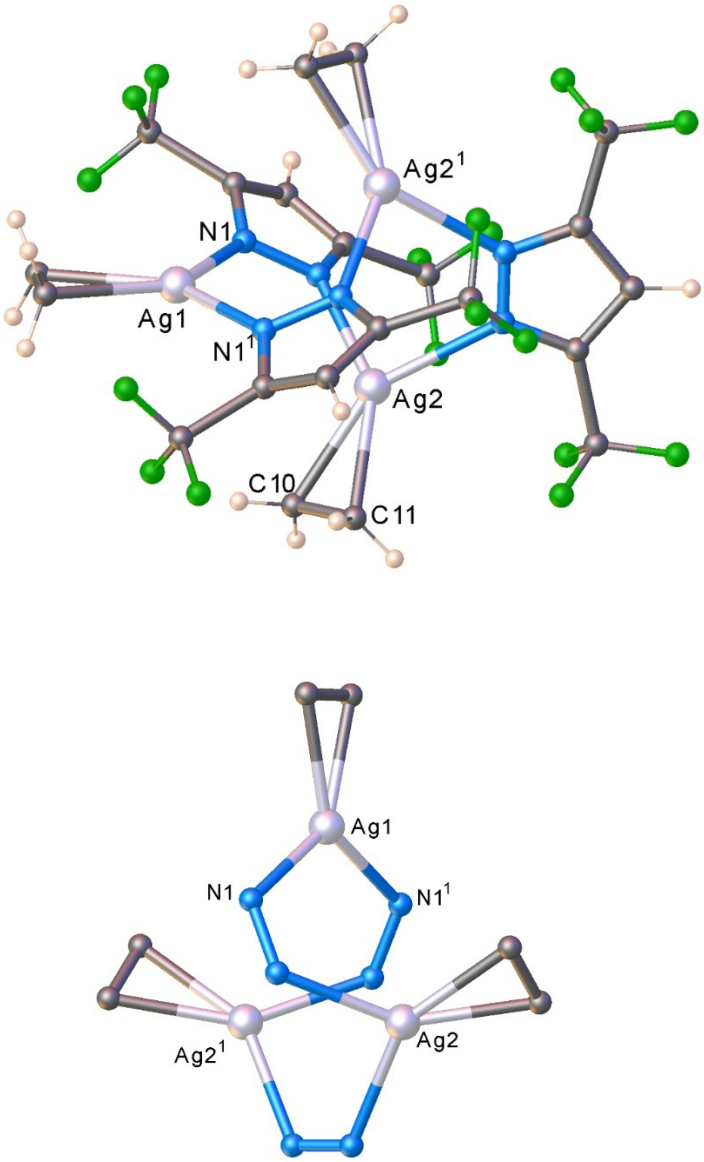


**Figure 4.** *In situ* PXRD based molecular structure of the silver-ethylene **[Ag-H•($C_2H_4$)]$_3$** intermediate generated by *in situ* solid-gas chemistry (top). Selected atoms showing only the $Ag_3N_6(C_2H_4)_3$ moiety and the distorted $Ag_3N_6$ core (bottom).

Postulating that this ethylene loaded trimer phase **[Ag-H•($C_2H_4$)]$_3$** might be a transition state between unloaded trimer and loaded dimer phases observed for other metal pyrazolates, experiments were carried out at even higher pressures and lower temperatures to see if a further transition to a loaded dimer "**[Ag-H•($C_2H_4$)]$_2$**" could be observed. First, the *in situ* PXRD data were collected at 45 bar of $C_2H_4$ from room temperature down to 110 K (just above the freezing point of $C_2H_4$). The pressure was then increased to 70 bar of ethylene and the sample warmed to room temperature (which led to **[Ag-H]$_3$** formation). We did not observe any evidence of new crystalline phase under both these conditions (see Figure S25).

Encouraged by the success with **[Ag-H]$_3$** that led to the characterization of a rare species in the ethylene bound yet pre trimer→dimer transformation stage, we also probed the chemistry of **[Ag-Br]$_3$** with ethylene. Note that these planar, trinuclear metal adducts display interesting and different extended structures and therefore, the outcome of solid-state chemistry with ethylene is not necessarily predictable through extrapolation. For example, in contrast to **[Ag-H]$_3$** which crystallizes forming zig-zag columns with argentophilic interactions,[9, 56] **[Ag-Br]$_3$**

trimers form extended structures with inter-trimer Ag···Br contacts[57] (while **[Ag-$CF_3$]$_3$** reported here shows inter-trimer Ag···F interactions between trimers).

Traditional solution chemistry with ~1 bar ethylene thus far did not yield an isolable silver-ethylene complex from **[Ag-Br]$_3$** in $CH_2Cl_2$. The *in situ* PXRD data of the solid-gas reaction of polycrystalline **[Ag-Br]$_3$** also do not show any phase changes even at 173K under flow of ethylene (~1 bar). However, at 10 bar of ethylene, a notable change was observed at 220K (Figure S26). Data analysis indicated that it directly progressed to the dimer stage producing {[4-Br-3,5-$(CF_3)_2$Pz]Ag($C_2H_4$)}$_2$ (**[Ag-Br•($C_2H_4$)]$_2$** (Figures 5 and S30), which is in contrast to the **[Ag-H]$_3$** chemistry but similar to that observed with **[Ag-$CF_3$]$_3$** and ethylene. Upon warming, **[Ag-Br•($C_2H_4$)]$_2$** loses ethylene and returns to the precursor trimer at 295K, even under 10 bar of ethylene (Figures S27 and S28). The dinuclear silver(I) ethylene complex **[Ag-Br•($C_2H_4$)]$_2$** adopts a slightly deeper a boat configuration with a closer Ag•••Ag separation (3.35(2) Å) within the six-membered $Ag_2N_4$ core relative to that observed with **[Ag-$CF_3$•($C_2H_4$)]$_2$** (which has Ag•••Ag separations at 3.49(2) Å). Ethylene ligands are $\eta^2$-bonded to silver sites, as expected. Overall, trinuclear **[Ag-Br]$_3$** and **[Ag-$CF_3$]$_3$** show unprecedented ethylene triggered solid-gas chemistry leading to dinuclear silver-ethylene complexes featuring $Ag_2N_4$ cores

while **[Ag-H]$_3$** enabled the observation of an ethylene bound silver trimer that retains the metalacyclic $Ag_3N_6$ core.

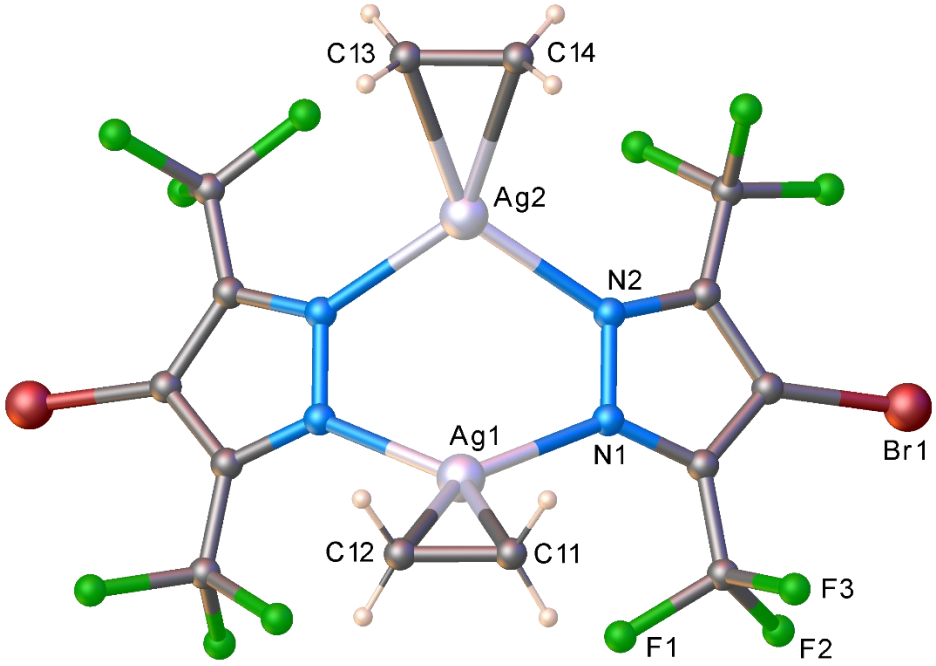


**Figure 5.** Molecular structure of *in situ* generated **[Ag-Br•($C_2H_4$)]$_2$** based on powder X-ray diffraction data.

***Computational study:*** In order to further understand ethylene driven molecular reorganization processes described above, we undertook a detailed computational study of ethylene reactions of **[Ag-$CF_3$]$_3$**, **[Ag-Br]$_3$** and **[Ag-H]$_3$** (Figure 6). The Gibbs free energy profiles at 298K were computed to uncover reaction paths at room temperature in the molecular calculations at the TZ2P/BP86-D3 level of theory. For

this purpose, thermodynamic quantities from vibrational frequencies accounting for enthalpy and entropy changes for the proposed reaction mechanism were obtained (see supporting information for additional details). As the first step (Figure 6, **1**), the formation of an adduct between the trinuclear silver pyrazolate and three molecules of $C_2H_4$ was predicted, prior to the deformation of the $Ag_3N_6$ core as a transition state (**TS1**), which is further relaxed to the intermediate **2** (such as **[Ag-H•($C_2H_4$)]$_3$**), The formation of **2** involves a computed Gibbs free energy (298.15 K) of -16.8, -15.9 and -13.7 kcal/mol, respectively (Table S10), in comparison to the initial reactants, for **[Ag-$CF_3$]$_3$**, **[Ag-Br]$_3$** and **[Ag-H]$_3$**. The observed deformation of the $Ag_3N_6$ core from precursors to the intermediates is not favored in the absence of ethylene, by about 50 kcal/mol (Table S7) for all the species, showing that such processes is driven exclusively by the initial coordination of $C_2H_4$ to the bare $Ag_3N_6$ core (step **1**). The process of forming **[Ag-R•($C_2H_4$)]$_3$** from **[Ag-R]$_3$** and gaseous ethylene (R = H, Br, $CF_3$) is not favorable entropically and can be influenced significantly by lower temperatures. Thus, intermediate **2** is more likely to be characterized, especially at lower temperature, as experimentally realized in this work in the reaction involving **[Ag-H]$_3$**.

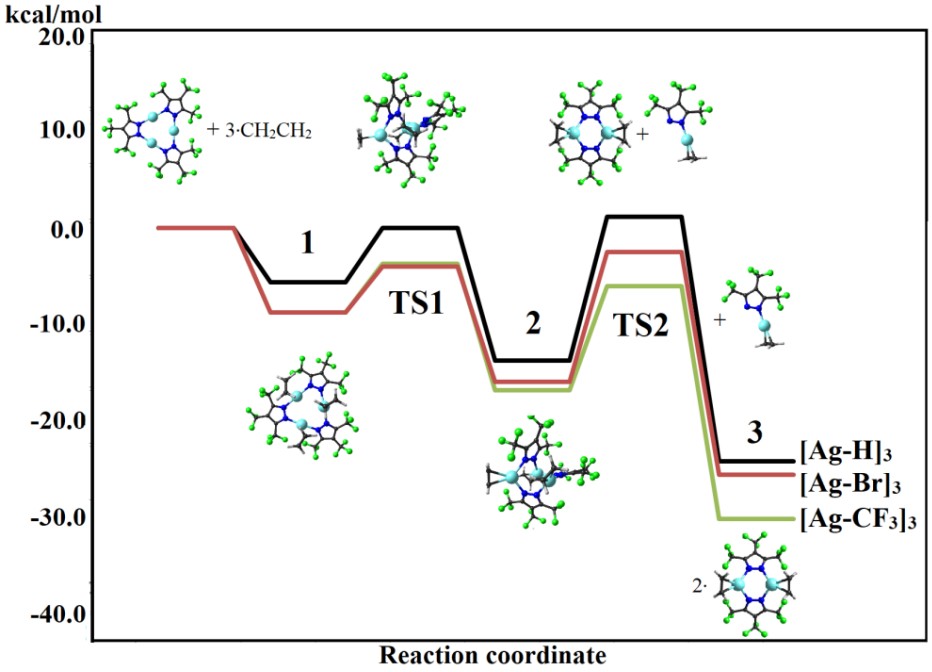


**Figure 6**. Gibbs free energy diagram for the proposed mechanism for dimer formation, involving **[Ag-H]$_3$**, **[Ag-Br]$_3$**, and **[Ag-CF$_3$]$_3$** at 298K. Values given per [Ag-R] unit in kcal/mol (R = H, Br, or $CF_3$).

Intermediate **2** is a key step prior to the trimer → dimer transformation. After the formation and relaxation of this intermediate, the next step is to release one **[Ag-R•(C$_2$H$_4$)]** unit (i.e., ethylene bound metal-pyrazolate) given as the second transition state (**TS2**), which is the rate-determinant step leading to the dimer. Calculations of the bonding energy of $Ag_2N_4$-$AgN_2$ (Table S8) for -H, -Br and -$CF_3$, indicate that it is easier to break-up **[Ag-CF$_3$]$_3$** and **[Ag-Br]$_3$** species (-64.3 and -65.2 kcal/mol, respectively), in comparison to **[Ag-H]$_3$** counterpart (-83.8 kcal/mol).

From the Gibbs free energy profiles (Table S9), the activation barriers related to the **1**→**TS1** process can be evaluated, which amount to 5.0, 4.7, and 5.6 kcal/mol for -$CF_3$, –Br, and –H at 298 K, respectively. For the **2**→**TS2** process, the related values are 10.8, 13.4, and 14.9 kcal/mol, denoting a slightly larger activation barrier for the **[Ag-H]$_3$** complex.

In the final step, the loss of a **[Ag-R•($C_2H_4$)]** unit from **[Ag-R•($C_2H_4$)]$_3$**, leads to the formation of one dimer species **[Ag-R•($C_2H_4$)]$_2$** (**TS2**), where the released unit further aggregates with another **[Ag-R•($C_2H_4$)]** fragment from a parallel reaction, resulting in the formation of a second dimer species (**3**). Calculated Gibbs free energy for step **3** amounts to -30.1, -25.5, and -24.1 kcal/mol for **[Ag-$CF_3$]$_3$**, **[Ag-Br]$_3$** and **[Ag-H]$_3$**, respectively. Overall, **[Ag-H•($C_2H_4$)]$_2$** formation is slightly less energetically favorable process, while **[Ag-$CF_3$•($C_2H_4$)]$_2$** formation is the most facile**,** which is consistent with the experimental observations, and denoted by the slightly less stabilized transition states and activation barriers, in addition to the bonding energy of $Ag_2N_4$-$AgN_2$ fragments prior formation of **TS2.** The formation of trinuclear-tris-ethylene intermediate **2** is favored at lower temperatures but the experimental conditions must be just right to trap this species before it breaks-up to even more energetically favorable dimers **3**. The silver(I) and $[3,5\text{-}(CF_3)_2Pz]^-$

ligand combination provides the ideal ingradients to trap the elusive species **[Ag-H•($C_2H_4$)]$_3$**.

## Conclusion

In summary, after a careful investigation that involved strategic variations of pyrazolyl ring substituents and solid-gas synthesis under different temperature-pressure combinations, and synchrotron based, *in situ* PXRD, we successfully trapped and structurally characterized a remarkable, trinuclear silver-ethylene complex {[3,5-($CF_3$)$_2$Pz]Ag($C_2H_4$)}$_3$ (**[Ag-H•($C_2H_4$)]$_3$**) with a severely distorted, yet intact $Ag_3N_6$ core, that can be viewed as a model for fleeting intermediates likely exist in ethylene driven, trimer-dimer transformations observed in related **[Ag-$CF_3$]$_3$** and **[Ag-Br]$_3$** systems. Furthermore, this study reveals for the first time, ethylene triggered structural transformations of trinuclear silver(I) pyrazolates in the solid-state leading to dinuclear species {[3,4,5-($CF_3$)$_3$Pz]Ag($C_2H_4$)}$_2$ (**[Ag-$CF_3$•($C_2H_4$)]$_2$**) and {[4-Br-3,5-($CF_3$)$_2$Pz]Ag($C_2H_4$)}$_2$ (**[Ag-Br•($C_2H_4$)]$_2$**), and molecular structures of two rare dinuclear, silver-ethylene complexes. This investigation also demonstrates the power of *in situ* synthesis over traditional solution chemistry for the isolation of labile species. Computational studies indicated that the silver(I)

and $[3,5\text{-}(CF_3)_2Pz]^-$ ligand combination provides the ideal ingradients to stabilize **$[Ag\text{-}H\bullet(C_2H_4)]_3$**. Further *in situ,* solid-gas studies guided by computational work in search of rare species from other metal complexes are currently underway.

## Supporting information

Details of the synthesis of **$[Ag\text{-}CF_3]_3$** and **$[Ag\text{-}CF_3\bullet(C_2H_4)]_2$** via solution methods, and the *in situ* solid phase synthesis of **$[Ag\text{-}CF_3\bullet(C_2H_4)]_2$**, **$[Ag\text{-}H\bullet(C_2H_4)]_3$** and **$[Ag\text{-}Br\bullet(C_2H_4)]_2$**, and the reverse processes, and molecular structure determinations using crystal X-ray crystallography and PXRD. Computational analysis of the ethylene uptake by silver pyrazolates, reaction pathways, additional figures, and references.

## Data availability

All data associated with this article can be found in the ESI.

## Conflicts of interest

There are no conflicts to declare.

**Acknowledgments.** This material is based upon work supported by the National Science Foundation under grant number (CHE-1954456, HVRD). A.M.-C. thanks the financial support from FONDECYT 1221676. Use of the Advanced Photon Source was supported by the U. S. Department of Energy, Office of Science, Office of Basic Energy Sciences, under Contract No. DE-AC02-06CH11357.

**Keywords**

Silver, Ethylene, Structure elucidation, Ligand effects, Pyrazolate

**References**

1. J. Zheng, Z. Lu, K. Wu, G.-H. Ning and D. Li, *Chem. Rev.*, 2020, **120**, 9675-9742.
2. J. Luo, X. Luo, M. Xie, H.-Z. Li, H. Duan, H.-G. Zhou, R.-J. Wei, G.-H. Ning and D. Li, *Nat. Commun.*, 2022, **13**, 7771.
3. R. Galassi, M. A. Rawashdeh-Omary, H. V. R. Dias and M. A. Omary, *Comments Inorg. Chem.*, 2019, **39**, 287-348.
4. J.-P. Zhang, Y.-B. Zhang, J.-B. Lin and X.-M. Chen, *Chem. Rev.*, 2012, **112**, 1001-1033.
5. J. Zheng, H. Yang, M. Xie and D. Li, *Chem. Commun.*, 2019, **55**, 7134-7146.
6. M. A. Omary, M. A. Rawashdeh-Omary, M. W. A. Gonser, O. Elbjeirami, T. Grimes, T. R. Cundari, H. V. K. Diyabalanage, C. S. P. Gamage and H. V. R. Dias, *Inorg. Chem.*, 2005, **44**, 8200-8210.

7. A. A. Titov, O. A. Filippov, L. M. Epstein, N. V. Belkova and E. S. Shubina, *Inorg. Chim. Acta*, 2018, **470**, 22-35.
8. R. Hahn, F. Bohle, W. Fang, A. Walther, S. Grimme and B. Esser, *J. Am. Chem. Soc.*, 2018, **140**, 17932-17944.
9. H. V. R. Dias, S. A. Polach and Z. Wang, *J. Fluor. Chem.*, 2000, **103**, 163-169.
10. H. V. R. Dias and C. S. Palehepitiya Gamage, *Angew. Chem. Int. Ed.*, 2007, **46**, 2192-2194.
11. M. A. Rawashdeh-Omary, M. D. Rashdan, S. Dharanipathi, O. Elbjeirami, P. Ramesh and H. V. R. Dias, *Chem. Commun.*, 2011, **47**, 1160-1162.
12. M. A. Omary, O. Elbjeirami, C. S. P. Gamage, K. M. Sherman and H. V. R. Dias, *Inorg. Chem.*, 2009, **48**, 1784-1786.
13. S.-Z. Zhan, F. Ding, X.-W. Liu, G.-H. Zhang, J. Zheng and D. Li, *Inorg. Chem.*, 2019, **58**, 12516-12520.
14. S.-K. Peng, Z. Lu, M. Xie, Y.-L. Huang, D. Luo, J.-N. Wang, X.-W. Zhu, X. Li, X.-P. Zhou and D. Li, *Chem. Commun.*, 2020, **56**, 4789-4792.
15. R. Liu, W. Zhang, D. Wei, J.-H. Chen, S. W. Ng and G. Yang, *Dalton Trans.*, 2019, **48**, 16162-16166.
16. H. Kestenbaum, A. Lange de Oliveira, W. Schmidt, F. Schüth, W. Ehrfeld, K. Gebauer, H. Löwe, T. Richter, D. Lebiedz, I. Untiedt and H. Züchner, *Ind. Eng. Chem. Res.*, 2002, **41**, 710-719.
17. J.-X. Liu, S. Lu, S.-B. Ann and S. Linic, *ACS Catal.*, 2023, **13**, 8955-8962.
18. R. H. Hertwig, W. Koch, D. Schröder, H. Schwarz, J. Hrušák and P. Schwerdtfeger, *J. Phys. Chem.*, 1996, **100**, 12253-12260.
19. H. V. R. Dias and C. J. Lovely, *Chem. Rev.*, 2008, **108**, 3223-3238.
20. J. Mehara, B. T. Watson, A. Noonikara-Poyil, A. O. Zacharias, J. Roithová and H. V. R. Dias, *Chem. Eur. J.*, 2022, **28**, e202103984.
21. M. S. Nechaev, V. M. Rayón and G. Frenking, *J. Phys. Chem., A*, 2004, **108**, 3134-3142.
22. K. Klimovica, K. Kirschbaum and O. Daugulis, *Organometallics*, 2016, **35**, 2938-2943.
23. I. Krossing and A. Reisinger, *Angew. Chem. Int. Ed.*, 2003, **42**, 5725-5728.
24. H. V. R. Dias and J. Wu, *Eur. J. Inorg. Chem.*, 2008, **2008**, 509-522.
25. Y. Yin, Z. Zhang, C. Xu, H. Wu, L. Shi, S. Wang, X. Xu, A. Yuan, S. Wang and H. Sun, *ACS Sustainable Chem. Eng.*, 2020, **8**, 823-830.
26. R. B. Eldridge, *Ind. Eng. Chem. Res.*, 1993, **32**, 2208-2212.
27. M. G. Cowan, W. M. McDanel, H. H. Funke, Y. Kohno, D. L. Gin and R. D. Noble, *Angew. Chem. Int. Ed.*, 2015, **54**, 5740-5743.

28. D. Parasar, A. H. Elashkar, A. A. Yakovenko, N. B. Jayaratna, B. L. Edwards, S. G. Telfer, H. V. R. Dias and M. G. Cowan, *Angew. Chem., Int. Ed.*, 2020, **59**, 21001-21006.
29. N. B. Jayaratna, M. G. Cowan, D. Parasar, H. H. Funke, J. Reibenspies, P. K. Mykhailiuk, O. Artamonov, R. D. Noble and H. V. R. Dias, *Angew. Chem., Int. Ed.*, 2018, **57**, 16442-16446.
30. K. A. Reid and D. C. Powers, *Chem. Commun.*, 2021, **57**, 4993-5003.
31. F. M. Chadwick, T. Krämer, T. Gutmann, N. H. Rees, A. L. Thompson, A. J. Edwards, G. Buntkowsky, S. A. Macgregor and A. S. Weller, *J. Am. Chem. Soc.*, 2016, **138**, 13369-13378.
32. F. M. Chadwick, A. I. McKay, A. J. Martinez-Martinez, N. H. Rees, T. Krämer, S. A. Macgregor and A. S. Weller, *Chem. Sci.*, 2017, **8**, 6014-6029.
33. J. C. Goodall, M. A. Sajjad, E. A. Thompson, S. J. Page, A. M. Kerrigan, H. T. Jenkins, J. M. Lynam, S. A. Macgregor and A. S. Weller, *Chem. Commun.*, 2023, **59**, 10749-10752.
34. E. Y. Slobodyanyuk, O. S. Artamonov, O. V. Shishkin and P. K. Mykhailiuk, *Eur. J. Org. Chem.*, 2014, **2014**, 2487-2495.
35. A. A. Mohamed, L. M. Pérez and J. P. Fackler, *Inorg. Chim. Acta*, 2005, **358**, 1657-1662.
36. H. V. R. Dias and H. V. K. Diyabalanage, *Polyhedron*, 2006, **25**, 1655-1661.
37. Y. Morishima, D. J. Young and K. Fujisawa, *Dalton Trans.*, 2014, **43**, 15915-15928.
38. H. V. R. Dias, Z. Wang and W. Jin, *Inorg. Chem.*, 1997, **36**, 6205-6215.
39. H. V. R. Dias and X. Wang, *Dalton Trans.*, 2005, 2985-2987.
40. H. A. Chiong and O. Daugulis, *Organometallics*, 2006, **25**, 4054-4057.
41. H. V. R. Dias, J. Wu, X. Wang and K. Rangan, *Inorg. Chem.*, 2007, **46**, 1960-1962.
42. A. Reisinger, N. Trapp and I. Krossing, *Organometallics*, 2007, **26**, 2096-2105.
43. S. Uchida, R. Kawamoto, H. Tagami, Y. Nakagawa and N. Mizuno, *J. Am. Chem. Soc.*, 2008, **130**, 12370-12376.
44. X. Kou and H. V. R. Dias, *Dalton Trans.*, 2009, 7529-7536.
45. A. Reisinger, N. Trapp, C. Knapp, D. Himmel, F. Breher, H. Rüegger and I. Krossing, *Chem. Eur. J.*, 2009, **15**, 9505-9520.
46. H. V. R. Dias and J. Wu, *Organometallics*, 2012, **31**, 1511-1517.
47. N. B. Jayaratna, I. I. Gerus, R. V. Mironets, P. K. Mykhailiuk, M. Yousufuddin and H. V. R. Dias, *Inorg. Chem.*, 2013, **52**, 1691-1693.

48. M. Stricker, B. Oelkers, C. P. Rosenau and J. Sundermeyer, *Chem. Eur. J.*, 2013, **19**, 1042-1057.
49. S. G. Ridlen, J. Wu, N. V. Kulkarni and H. V. R. Dias, *Eur. J. Inorg. Chem.*, 2016, **2016**, 2573-2580.
50. M. Navarro, J. Miranda-Pizarro, J. J. Moreno, C. Navarro-Gilabert, I. Fernández and J. Campos, *Chem. Commun.*, 2021, **57**, 9280-9283.
51. M. Vanga, A. Muñoz-Castro and H. V. R. Dias, *Dalton Trans.*, 2022, **51**, 1308-1312.
52. B. T. Watson, M. Vanga, A. Noonikara-Poyil, A. Muñoz-Castro and H. V. R. Dias, *Inorg. Chem.*, 2023, **62**, 1636-1648.
53. M. Fianchini, C. F. Campana, B. Chilukuri, T. R. Cundari, V. Petricek and H. V. R. Dias, *Organometallics*, 2013, **32**, 3034-3041.
54. H. V. R. Dias and M. Fianchini, *Angew. Chem. Int. Ed.*, 2007, **46**, 2188-2191.
55. I. I. Gerus, R. X. Mironetz, I. S. Kondratov, A. V. Bezdudny, Y. V. Dmytriv, O. V. Shishkin, V. S. Starova, O. A. Zaporozhets, A. A. Tolmachev and P. K. Mykhailiuk, *J. Org. Chem.*, 2012, **77**, 47-56.
56. H. Schmidbaur and A. Schier, *Angew. Chem. Int. Ed.*, 2015, **54**, 746-784.
57. C. V. Hettiarachchi, M. A. Rawashdeh-Omary, D. Korir, J. Kohistani, M. Yousufuddin and H. V. R. Dias, *Inorg. Chem.*, 2013, **52**, 13576-13583.